J. Fluid Mech. (1988), *vol.* 197, *pp.* 415–427
Printed in Great Britain

Gravity–capillary rings generated by water drops

By BERNARD LE MÉHAUTÉ

Division of Applied Marine Physics, Rosenstiel School of Marine and Atmospheric Science, University of Miami, Miami, FL 33149, USA

(Received 16 February 1988 and in revised form 17 May 1988)

A theory for water waves created by the impact of small objects such as raindrops on an initially quiescent body of water is established. Capillary and dissipative viscous effects are taken into account in addition to gravity. It is shown that the prevailing waves are in a mixed capillary–gravity regime around a wavenumber k_m which corresponds to the minimum value of the group velocity. The waves are described as function of time and distance by the linear superposition of two transient wave components, a 'sub-k_m' ($k < k_m$) component and a 'super-k_m' ($k > k_m$) component. The super-k_m components prevail at a short distance from the drop, whereas only the sub-k_m ones remain at a larger distance. The relative time history of the wavetrain is independent of the size of the drop, and its amplitude is proportional to the drop momentum when it hits the free surface. The wave pattern is composed of a multiplicity of rings of amplitude increasing towards the drop location and is terminated by a trailing wave with an exponential decay. The number of rings increases with time and distance.

1. Introduction

The rings formed by raindrops in a pond, or by the fall of any tiny object, are a natural fascinating phenomenon which is commonly observed. However, its tiny scale, its transient nature and its relative complexity, has prevented the casual observer from describing it in its intricate details. It was not until high-speed photography could be used that one was able to visualize the small capillary crown created at the drop location, evolving into the more conspicuous expanding rings vanishing slowly away.

Surprisingly, such a common phenomenon has little inspired hydrodynamicists. It seems that only Crapper (1984) has mentioned the subject: his figure 5.5, p. 115, showing a photograph of the rings caused by raindrops of different size at several different times. Lately, the subject matter has become more pertinent, in view of the effects that gravity–capillary rings generated by raindrops have on radar (and even sonar) returns in the frequency range of interest. In addition, the inception and damping of wind waves, the exchange of interface momentum, the rate of turbulence and mixing processes, and the breaking of surface films, are all phenomena that are influenced by raindrops and their subsequent gravity–capillary rings.

From a theoretical point of view, this phenomenon belongs to the family of impulsively generated water waves which has been investigated frequently in the past in regard to tsunami and explosion-generated water waves (Kranzer & Keller 1951; Kajiura 1963; Le Mehaute 1970). However, the capillary and viscous dissipative effects, which have been neglected in the past, are now of primary importance.

The purpose of this paper is to present a theoretical treatment of the gravity–capillary rings generated by a raindrop in a liquid, allowing us to explain and describe a number of commonly observed physical phenomena. The investigation is limited to linear approximations, which limit its validity at the origin. The viscous damping resulting from the free-surface boundary layer due to surface film contamination is introduced as a correction to the non-dissipative irrotational main flow as done by Dorrestein (1951) in the case of monochromatic one-dimensional wave. Whether the rain itself breaks the surface film and subsequently modifies the wave damping, as suggested by Van Dorn (1966), remains an open question.

Initially, a general dimensionless mathematical model for axisymmetric irrotational free-surface flow is recalled. Then initial boundary conditions related to the raindrop are introduced. Analytical solutions are presented and the results are analysed, with emphasis on the effect of dispersion in the mixed capillary–gravity regime and the trailing wave.

2. Establishment of the equations of motion

The motion is defined with respect to time t^* and space (r^*, z^*, θ^*) in a cylindrical coordinate system centred at the impact spot of the drop. The horizontal radial distance is r^*, and the vertical distance z^* is positive upwards from the still water level, an asterisk denoting dimensional quantities. The motion is symmetrical with respect to the z-axis. For all practical purposes, the water depth is infinite relative to the wavelengths generated by the drop and this is assumed.

Initially, neglecting the dissipative processes at the fall location and in the thin near-surface viscous boundary layer, the motion is assumed to be irrotational, allowing the definition of a potential function $\phi^*(r^*, z^*, t^*)$ with a free surface $\eta^*(r^*, t^*)$.

The motion is non-dimensionalized with respect to a horizontal distance R^*, which characterizes the size of the initial disturbance. The following dimensionless quantities are now defined (g is the gravitational acceleration):

$$(r, z, \eta) = \frac{r^*, z^*, \eta^*}{R^*}, \quad t = t^*\left(\frac{g}{R^*}\right)^{\frac{1}{2}}, \quad \phi = \frac{\phi^*}{(gR^{*3})^{\frac{1}{2}}}. \tag{1}$$

Also, ρ is the water density (1 g/cm^3), τ^* the surface tension per unit area, σ^* the frequency and k^* the wavenumber, and

$$\tau = \frac{\tau^*}{\rho g R^{*2}}, \ (\tau^* \approx 74 \text{ dynes/cm}), \quad \sigma = \sigma^*\left(\frac{R^*}{g}\right)^{\frac{1}{2}}, \quad k = k^*R^*. \tag{2}$$

The solution satisfies continuity. The linearized boundary condition at the free surface includes an additional term due to surface tension, so that

$$\phi_t = -\eta + \tau\left[\eta_{rr} + \frac{1}{r}\eta_r\right], \tag{3}$$

which gives the same free-surface condition as found for plane waves. Accordingly, the general solution is obtained by a continuous linear superposition of wave components characterized by a wavenumber k such as given by (see Lamb 1932)

$$\phi(r, z, t) = \int_0^\infty J_0(kr)\, \mathrm{e}^{-kz}\, [A(k) \sin \sigma t + B(k) \cos \sigma t]\, k \, \mathrm{d}k \tag{4}$$

and
$$\eta(r, t) = \int_0^\infty J_0(kr)\,[A(k)\cos\sigma t - B(k)\sin\sigma t]\,\sigma k\,\mathrm{d}k. \tag{5}$$

The coefficients $A(k)$ and $B(k)$ are defined from initial free-surface conditions imposed by the raindrops. The dispersion relationship is

$$\sigma^2 = k[1+\tau k^2]. \tag{6}$$

The initial conditions are defined by an impulse on the free surface over a radius R^*, which can be considered as being equal to the drop radius, as a first approximation. Assuming that the water drop movement following the impact is negligible, the total impulse I_t^* on the free surface is equal to the drop momentum M^*W^*, where M^* is its mass and W^* its fall velocity, so that in dimensionless terms
$$I_t = \frac{M^*}{\rho R^3}\frac{W^*}{(gR^*)^{\frac{1}{2}}} \approx \frac{4\pi}{3}W. \tag{7}$$

Furthermore, if one assumes that the drop is spherical and reaches terminal velocity before impact, then, in the case of a drop larger than 1 mm in radius,

$$I_t = \frac{4\pi}{3}\left(\frac{8}{3\,C_x}\frac{\rho}{\rho_a}\right)^{\frac{1}{2}} \left(\approx 273.61\right), \tag{8}$$

where C_x (the drag coefficient) ≈ 0.5 and the density ratio ρ/ρ_a of water to air is 800. It has been known for a long time that large drops are not quite spherical and that the drop size is practically limited by the pressure forces to a maximum value of $R^* \approx 4.0$ mm (Horton 1947; Gunn & Kinzer 1949; and Lhermitte 1971).

This total impulse is equal to the sum of the pressure distribution $p(r_0, \theta)$, where r_0 is r within the limits of the initial disturbance:
$$I_t = \int_0^{2\pi}\int_0^1\int_{t_0} p(r_0, \theta)\,\delta(t-t_0)\,\mathrm{d}t\,r_0\,\mathrm{d}r_0\,\mathrm{d}\theta, \tag{9}$$

where δ is a Dirac delta function and t_0 is the time when the drop reaches the free surface.

The pressure distribution $p(r_0, \theta)$ is loosely related to the kinetic energy and mass distribution. It is assumed that
$$p(r_0, \theta) = p_{\max}(1-r_0^2)^n. \tag{10}$$

For a spherical mass distribution prior to impact $n = \frac{1}{2}$. We assume $n = 1$, however, corresponding to a parabolic distribution, for the sake of mathematical convenience. (It is found that the results are not sensitive to the exact form of the pressure distribution.) Accordingly, combining (7), (9) and (10), the initial condition at the free surface in term of ϕ can be written as
$$\phi(r_0, t_0) = \tfrac{8}{3}W(1-r_0^2), \quad r_0 \leqslant 1. \tag{11}$$

Referring to (4) where $z = \eta \approx 0$ and $t = t_0 = 0$, yields $A(k) = 0$ and
$$\tfrac{8}{3}W(1-r_0^2) = \int_0^\infty J_0(kr)\,B(k)\,k\,\mathrm{d}k. \tag{12}$$

Equation (12) can be inverted by virtue of the Fourier–Bessel theorem. Then
$$B(k) = \tfrac{8}{3}W\int_0^1 J_0(k\,r_0)\,(1-r_0^2)\,r_0\,\mathrm{d}r_0, \tag{13}$$

which is a Hankel transform that can be integrated analytically:

$$B(k) = \tfrac{8}{3} W \frac{2}{k^2} J_2(k). \tag{14}$$

Inserting (14) into (15) and defining

$$\theta(r, t) = \frac{3}{16} \frac{\eta(r, t)}{W} = \frac{3\eta^*(r, t)}{16R^*} \frac{(gR^*)^{\frac{1}{2}}}{W^*} \tag{15}$$

finally gives

$$\theta(r, t) = \int_0^\infty \frac{\sigma}{k} J_2(k) J_0(kr) \sin \sigma t \, \mathrm{d}t, \tag{16}$$

where σ is given as function of k by the dispersion relationship (6). Reverting to dimensional quantities,

$$\frac{3}{16} \frac{\eta^*}{R^*} \frac{(gR^*)^{\frac{1}{2}}}{W^*} = \left(\frac{R^*}{g}\right)^{\frac{1}{2}} \int_0^\infty \frac{\sigma^*}{k^*} J_2(k^*R^*) J_0(k^*r^*) \sin \sigma^* t^* \, \mathrm{d}k^*. \tag{17}$$

Since k^*R^* is small for the waves under consideration as seen in the following, J_2 can be replaced by

$$J_2(k^*R^*) \approx \tfrac{1}{2}(\tfrac{1}{2}k^*R^*)^2 \tag{18}$$

so that

$$\frac{3}{2} \frac{g\eta^*(r^*, t^*)}{R^{*3}W^*} = \frac{6\pi\rho g\eta^*}{M^*W^*} = \int_0^\infty \sigma^* k^* J_0(k^*r^*) \sin \sigma^* t^* \, \mathrm{d}k^*. \tag{19}$$

Dividing the integral (19) (dimension $L^{-2}T^{-1}$) by $\sigma_m^* k_m^{*2}$, a universal dimensionless solution is obtained. The relative time history, with maxima, minima and zero crossing, of the free-surface elevation is independent of the size of the original disturbance. Also, it shows that the amplitudes are proportional to the drop momentum M^*W^* or, equivalently, proportional to $R^{*3}W \approx R^{*3.5}$. The fact that the relative time history of the free-surface elevation is independent of the size of the initial disturbance for the type of waves under consideration, but depends only upon the fluid characteristics and gravity (ρ, τ^*, g) is an interesting fact which is not confined to parabolic disturbances. It is a property of all small disturbances of the free surface. For example the Hankel transform of a disturbance with a uniform distribution is $(R/k) J_1(kR)$, that of a parabolic disturbance with lip is $(R/k) J_3(kR)$, and that of a quadratic disturbance is $(4/k^2) J_4(kR)$. As long as (kR) remains small, all these Bessel functions can be replaced by the first terms of their power expansion, which gives $R^2/2$, $R^4k^2/48$, $R^4k^2/96$ respectively. All these functions allow us to extract the R-function from the integral, influencing only the wave amplitude and independent of frequency.

3. Analytical solution

In the general case (16) cannot be integrated analytically. However at the point of impact $J_0(kr) = 1$. Then it has been found analytically in the non-dispersive case ($\sigma = k$) and numerically in the deep-water case ($\sigma = k^2$), that the movement at the point of impact is non-oscillatory (Le Mehaute, Wang & Lu 1987). This means that the multiplicity of rings that are observed at a distance are solely the results of linear dispersion from the initial non-oscillatory movement. The movement at the drop location calms down very rapidly following a unique rapid down and up oscillation ($\theta < 0.1$, when $t^* = 2(gR)^{\frac{1}{2}} \approx 0.20$ to 0.40 s). This can also be observed by throwing a

rock into an initially quiescent body of water. The only movement that is observed is the multiplicity of circular rings radiating outwardly, whereas the free surface at the point of impact calms down very rapidly. Therefore, practically no energy radiates from the point of impact after a very short time following the initial contact of the drop with the initially quiescent liquid, a fact which will be used in the following treatment of the trailing wave.

At a short distance (a few cm) when $kr \gg 1$, $J_0(kr)$ can be replaced by the first term of its asymptotic expansion and the stationary phase approximation can be used. Using standard procedures (Jeffreys & Jeffreys 1956), one finds after some arithmetic

$$\theta(r, t) = \frac{1}{r}\frac{\sigma}{k^2}J_2(k)\left(\frac{kV}{|-\mathrm{d}V/\mathrm{d}k|}\right)^{\frac{1}{2}}\sin(\sigma t - kr), \tag{20}$$

where

$$\frac{r}{t} = \frac{\mathrm{d}\sigma}{\mathrm{d}k} = V(k) = \frac{1+3\tau k^2}{2k^{\frac{1}{2}}(1+\tau k^2)^{\frac{1}{2}}} \tag{21}$$

is the group velocity (Crapper 1984). Therefore the solution appears as a sinusoid in terms of r or t, modulated in amplitude by a function of k.

Recall V is minimum ($V = V_\mathrm{m}$) when

$$\frac{\mathrm{d}V}{\mathrm{d}k} = \frac{\mathrm{d}^2\sigma}{\mathrm{d}k^2} = -\frac{3(\tau k^2)^2+6\tau k^2-1}{4k^{\frac{3}{2}}(1+\tau k^2)^{\frac{3}{2}}} = 0, \tag{22}$$

i.e. when

$$\tau k^2 = \tau k_\mathrm{m}^2 = 0.1547\left(=\frac{\tau^* k^{*2}}{\rho g}\right), \tag{23}$$

$$k_\mathrm{m} = 0.3933\tau^{-\frac{1}{2}}. \tag{24}$$

Accordingly, $V_\mathrm{m}^* = 17.9$ cm/s and $k_\mathrm{m}^* = 1.432$ cm^{-1}, corresponding to a wavelength of $L_\mathrm{m}^* = 4.39$ cm. It is also seen that the energy travels at the same velocity V^* for two different values of k^*, which implies that the wave motion at a given (r^*, t^*)-value is the sum of two wave components with different transient frequencies.

The existence of a minimum group velocity V_m and the fact that the motion at the drop location is nearly instantaneous, as shown in the previous section, implies that the free surface is still over an area limited by a radius $r_\mathrm{m}^* = V_\mathrm{m}^* t^*$, a fact also noted by Crapper (1984). Also, recall that the group velocity exceeds the phase velocity when $\tau k^2 > 1$ and tends towards $\frac{3}{2}$ c when $k \to \infty$, whereas it tends towards $\frac{1}{2}c$ when $k \to 0$. When $\mathrm{d}V/\mathrm{d}k$ is zero, the stationary phase approximation is no longer valid, as discussed below.

4. Insertion of dissipative processes and results

An active dissipative process, corresponding to the drop deformation and mixing, exists at the drop location, but momentum is conserved. At a distance, the dissipation process in deep water is due to the surface boundary layer which results from contamination of the surface (Dorrenstein 1951; Van Dorn 1966). Also, there is dissipation resulting from the straining of irrotational motion, which induces a streaming motion due to the second-order mean velocity field. This effect is germane in regard to mass transport and momentum balance (Phillips 1966).

In both cases, a damping coefficient $D(k^*)$ is given by

$$D(k^*) = \exp[-\gamma_\nu^* t^*], \tag{25}$$

where, in the case of a fully contaminated surface,

$$\gamma_{\nu 1}^* = \tfrac{1}{2}\nu\left(\frac{\sigma^*}{2\nu}\right)^{\frac{1}{2}} k^* \tag{26}$$

and ν is the kinematic viscosity.

The damping due to internal strain is given by

$$\gamma_{\nu 2}^* = 2\nu k^{*2}. \tag{27}$$

Inserting (20), where J_2 is replaced by (18), the dimensional solution to the problem is finally given by

$$\frac{3}{2}\frac{g\eta^*(r^*, t^*)}{r^{*3}W^*} = \frac{\sigma^*}{r^*}\left(\frac{k^*V^*}{|-\mathrm{d}V^*/\mathrm{d}k^*|}\right)^{\frac{1}{2}} D(k^*)\sin(\sigma^* t - k^* r^*), \tag{28}$$

where

$$V^*(k^*) = \frac{\mathrm{d}\sigma^*}{\mathrm{d}k^*} = \frac{r^*}{t^*} \tag{29}$$

and

$$\sigma^* = \left[gk^*\left(1 + \frac{\tau^* k^{*2}}{\rho g}\right)\right]^{\frac{1}{2}}. \tag{30}$$

The analytical results corresponding to the previous formulation is given in figure 1 (a, b, c) showing

$$Y(r^*, t^*)\,(\mathrm{cm}^{-2}, \mathrm{s}^{-1}) = \frac{3}{2}\frac{g\eta^*(r^*, t^*)}{R^{*3}W^*} = \frac{6\pi\rho g\eta^*(r^*, t^*)}{M^*W^*} \tag{31}$$

in terms of the right-hand side of (28). The results are initially presented in terms of t^* for fixed values of r^* (30, 60, 120 cm) in the case of a contaminated free surface (equation (26)). For each value of r^* there is a corresponding limit maximum time $t^* = r^*/V_{\mathrm{m}}^*$ of the trailing wave, after which the free-surface elevation tends to zero as seen in the following. The two components of the waves, sub-k_{m}, where $k < k_{\mathrm{m}}$, and super-k_{m}, where $k > k_{\mathrm{m}}$, are presented on two separate horizontal axis (Y_{G}, Y_{C}). The total wave movement is given on a top third axis Y, given by the linear superposition of the two wave components.

It is observed that the super-k_{m} components precede and initially hide the sub-k_{m} components (figure 1a), but they are damped rapidly with distance, where only the sub-k_{m} components remain (figure 1c). At the origin most of the energy is imparted to waves of very high frequency, but, at a short distance (2–3 cm), the prevailing apparent frequencies are in the mixed capillary–gravity regime. Indeed, the drop sizes (which intervene theoretically in $J_2(k^*R^*)$) are generally too small to impart a significant amount of energy in the 'pure' gravity regime, and the wave damping at high frequency is too effective for the 'pure' capillary waves, so that they can be observed near the drop location only.

In the case where the energy dissipation process is limited to viscous strain (equation (27)), then the sub-k_{m} wave components prevail at a much longer distance as seen in figure 2.

If one neglects energy dissipation altogether (figure 3), then one can see that the wave height in the sub-k_{m} regime increases with time to a maximum value

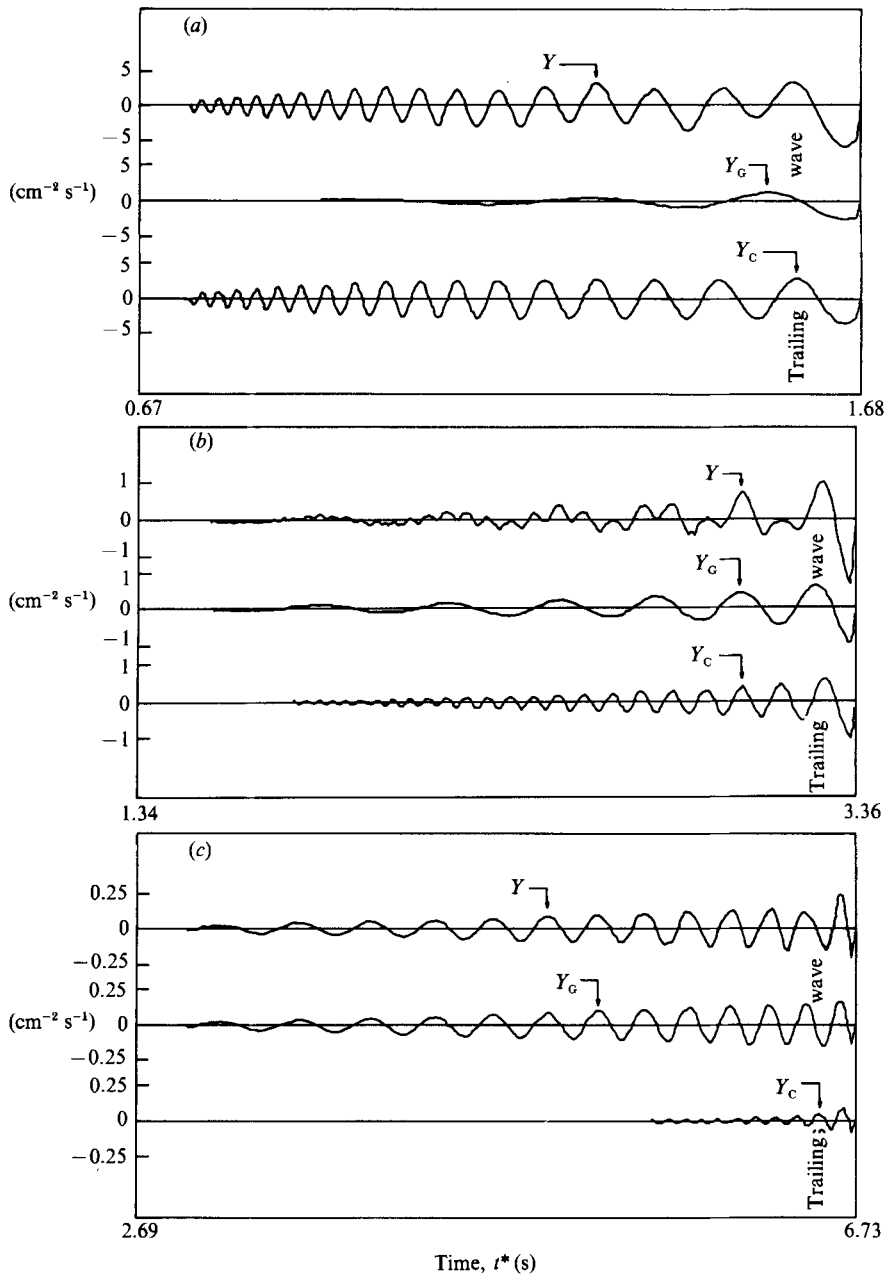

FIGURE 1. Functions $Y(t^*)$ *vs.* time t^* at three distances r^* from the drop ((*a*) 30, (*b*) 60, (*c*) 120 cm) in the case of a contaminated free surface. Sub-k_m components: Y_C; super-k_m^* components: Y_G; and $Y = Y_G + Y_C$. Note the differences in scales.

corresponding to the maximum of $J_2(k^*R^*)$. This is logical since it is expected that most of the energy is initially imparted to wavelengths of the order of $2R^*$. (The maximum of J_2 is for $k^*R^* = 3.1$, corresponding to a wavelength $L^* = 2\pi R^*/3.1 \approx 2.02R^*$). The importance of the dissipation process for an accurate prediction of wave amplitude and wave steepness is then appreciated.

In another form of presentation, the results are given at a fixed time t^* as function

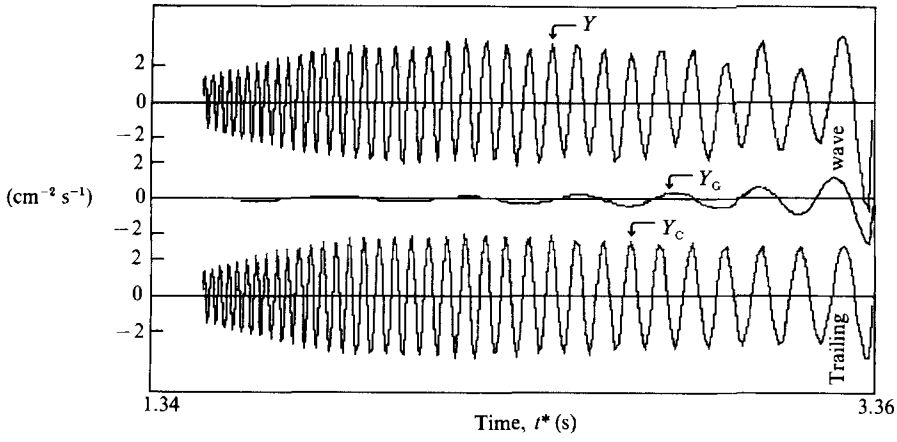

FIGURE 2. Functions $Y(t^*)$ *vs.* time t^* at a distance $r^* = 60$ cm in the case of damping by internal viscous strain alone.

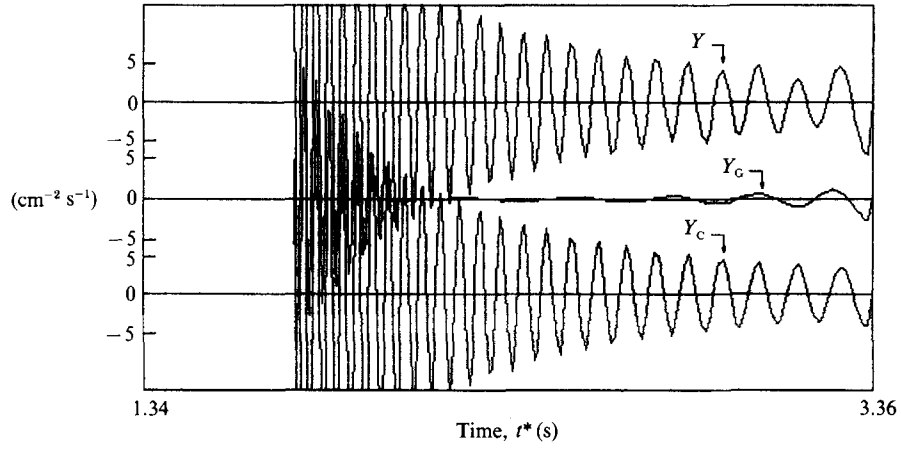

FIGURE 3. Functions $Y(t^*)$ at a distance $r^* = 60$ cm from the drop in the case where viscous dissipation is neglected.

of the horizontal distance r^* in the case of a fully contaminated surface (equation (26)). Then t^* is replaced by r^*/V^* in (28). The results are given for the near field ($0 < r^* < 100$ cm) (figure 4*a*) and for the far field ($0 < r^* < 300$ cm) (figure 4*b*). In these figures, only the sum of the two components is presented. One sees that at an early time after the drop, the super k_m^* components hide the sub-k_m^* components. Later as the wave travels away, the only signature of the drop are the sub-k_m^* components, whereas the super-k_m^* ones have virtually vanished.

5. The mixed capillary–gravity regime

The pure capillary and pure gravity regimes correspond to the cases where $\tau k^2 \gg 1$ and $\tau = 0$, respectively. For the problem under consideration, in the frequency range of interest, the problem belongs to the mixed capillary–gravity regime. Since high-frequency waves are rapidly damped, and since too little energy is imparted to the lower frequency, it happens that for practical purposes, the energy spectrum is centred around k_m (or σ_m), corresponding to the minimum group velocity V_m.

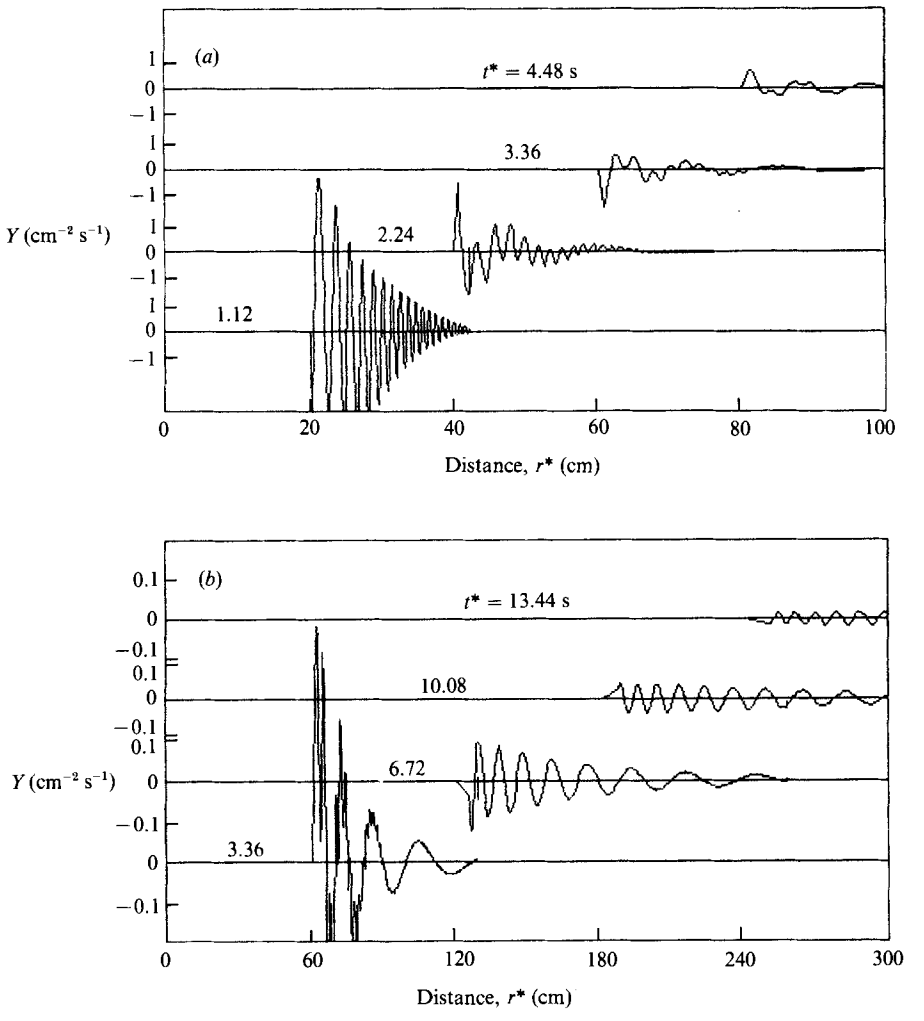

FIGURE 4. Successive form of functions $Y(r^*)$ at 4 time intervals for (*a*) the near field (0–1 m) and (*b*) the far field (0–3 m). (Note the difference in vertical scales on the two curves at $t^* = 3.36$ s).

A mixed capillary–gravity regime is defined between the pure capillary and the pure gravity regimes around k_m. Since $d^2\sigma/d_m^2 = 0$ at $k = k_m$, the local frequency variations are given by

$$\sigma = \sigma_m + \frac{d\sigma_m}{dk}(k-k_m) + \frac{1}{6}\frac{d^3\sigma_m}{dk_m^3}(k-k_m)^3, \tag{32}$$

or, as a first approximation, $$\sigma \approx \sigma_m + V_m(k-k_m), \tag{33}$$

which gives $$\sigma = 1.086k\tau^{\frac{1}{4}} + 0.2468\tau^{-\frac{1}{4}}. \tag{34}$$

A systematic comparison of the values of σ^*, phase and group velocity (C^*, V^*) in the general case when both gravity and capillarity are taken into account, on one hand, and their asymptotic forms established for the pure capillary, the pure gravity and also the mixed regimes as defined by (34), on the other hand, yields their optimum ranges of validity which are given by table 1.

It is seen that the mixed regime such as defined by (33) covers a broad range

	Capillary	Max error σ^*, C^* 13%	Mixed	Max error σ^*, C^* 1.7%	Gravity
L^* (cm)	$L^* < 1.2$	$L^* = 1.2$	$1.2 < L^* < 8.8$	$L^* = 8.8$	$L^* > 8.8$
T^* (s)	$T^* > 0.05$	$T^* = 0.05$	$0.05 < T^* < 0.23$	$T^* = 0.23$	$T^* > 0.23$
k^* (cm^{-1})	$k^* > 5.23$	$k^* = 5.23$	$5.23 > k^* > 0.70$	$k^* = 0.7$	$k^* < 0.70$
σ^* (s^{-1})	$\sigma^* > 125$	$\sigma^* = 125$	$125 > \sigma^* > 27$	$\sigma^* = 27$	$\sigma^* < 27$

TABLE 1. Optimum ranges of validity of frequency, and phase and group velocities

of values, which are most pertinent to the problem under investigation. The accuracy of (34) is within 1% between $2.41 > k^* > 0.80$ and within 0.1% between $1.95 > k^* > 1.00$.

It can be concluded that waves generated by liquid drops belong to the mixed regime around the minimum group velocity values ($k_m^* = 1.43$ cm^{-1}, $L_m^* = 4.39$ cm), for which the dispersion relationship is given by (33). In this respect these waves are nearly non-dispersive in the sense that σ is linearly related to k, and the group velocity varies little with frequency.

6. The trailing wave

When $d^2\sigma/dk^2 \to 0$, and $V \to V_m$, the value of η^* given by (28) tends to infinity. Then the stationary phase approximation is no longer valid. A locally valid solution can be obtained by making use of (32), by analogy with the leading wave of a tsunami (Whitham 1974). Replacing J_0 by the first term of its asymptotic form, (16) becomes

$$\theta(r, t) = \int_0^\infty F(k) \exp[\mathrm{i}(\sigma t - kr + \tfrac{1}{4}\pi)]\,\mathrm{d}k, \tag{35}$$

where

$$F(k) = \frac{\sigma}{k} J_2(k) \left(\frac{1}{\pi k r}\right)^{\frac{1}{2}}. \tag{36}$$

Inserting the value of σ given by (33) into (35), and replacing $F(k)$ by $F(k_m)$ yields

$$\theta(r, t) = F(k_m) \int_{-k_m}^\infty \exp \mathrm{i}\,[(\sigma_m + V_m K)t - kr + \gamma K^3 t + \tfrac{1}{4}]\,\mathrm{d}k, \tag{37}$$

where

$$K = k - k_m \tag{38}$$

and

$$\gamma = \frac{1}{6}\frac{\mathrm{d}^3\sigma_m}{\mathrm{d}k_m^3} = \frac{3\tau k_m^2}{k_m^{\frac{5}{2}}(1+\tau k_m^2)^{\frac{1}{2}}} = 4.452\tau^{\frac{5}{4}}. \tag{39}$$

Adding and subtracting $k_m r$ to the argument and since the integral is valid only locally ($k \approx k_m$), $\theta(r, t)$ can still be written

$$\theta(r, t) = F(k_m) \exp \mathrm{i}\,(\sigma_m t - k_m r + \tfrac{1}{4}\pi) \int_{-\infty}^\infty \exp \mathrm{i}\,[K(V_m t - r) + \gamma K^3 t]\,\mathrm{d}K. \tag{40}$$

Changing variables as follows:

$$s = \frac{(3\gamma t)^{\frac{1}{3}}}{K}, \tag{41}$$

$$z = \frac{V_m t - r}{(3\gamma t)^{\frac{1}{3}}}, \tag{42}$$

gives

$$\theta(r, t) = F(k_m) \cos k_m (V_m t - r + \tfrac{1}{4}\pi) \int_0^\infty \cos (sz + \tfrac{1}{3}s^3)\, ds. \tag{43}$$

Dividing the integral by π, an Airy function Ai (z) is obtained. Therefore one has finally

$$\theta(r, t) = F(k_m) \cos k_m (V_m t - r + \tfrac{1}{4}\pi)\, \pi\, \mathrm{Ai}\,(z). \tag{44}$$

Note that this solution is nearly identical to the case of a leading gravity wave (Whitham 1974), except that the Airy function is now the envelope of the cos function instead of being the free-surface elevation.

At the trailing edge when $r = V_m t$, then (Abramovitz & Stegun 1965),

$$\mathrm{Ai}\,(0) = 3^{-\frac{2}{3}}/\Gamma(\tfrac{2}{3}) = 0.355, \tag{45}$$

so that

$$\theta(r_m, t_m) = 0.335\pi\, F(k_m) \cos(\tfrac{1}{4}\pi\, k_m), \tag{46}$$

which is finite.

It is recalled that when z is large and positive ($r < V_m t$), Ai (z) decays rapidly and becomes negligible when $z \approx 2$ (as does θ). When z is large and negative ($r > V_m t$), Ai (z) exhibits oscillatory behaviour which decreases in amplitude as z increases. As $r \gg V_m t$, the solution merges with the stationary wave solution as shown by Whitham (1974). It can be concluded from the form of the Airy function as well as from the stationary phase solution that the trailing wave is the largest wave. The elevation of the free surface at $r^* = V_m t^*$ is not nil and is given by (46).

7. Conclusions

A theory for water waves generated by the fall of tiny objects such as raindrops on an initially quiescent body of water has been established. Most theoretical features that have been found are well illustrated in the previously mentioned photograph presented by Crapper (1984). Our main conclusions are:

(i) Such waves belong to the mixed capillary–gravity regime, between pure capillary waves and pure gravity waves. These waves obey, as a first order of approximation, a linear relationship between frequency and wavenumber (equation (33)). The group velocity varies little with frequency.

(ii) The multiplicity of rings observed at a distance from the drop is solely the result of dispersion from a unique oscillation taking place at the drop location.

(iii) These waves have a narrow range of wavenumbers around k_m^*, the wavenumber that corresponds to the minimum possible group velocity V_m^*.

(iv) The relative time history of the free-surface elevation (zero crossing, and locations of maxima and minima) is given solely as a function of time t^* and distance r^*, as a function of the fluid characteristics τ^*, ρ and to a first approximation g, and does not depend upon the size R^* nor velocity W^* of the drop. (This would not be valid for original disturbances of larger sizes.)

(v) The free-surface elevation at a given time t^* or distance r^* (such as $r^* > V_m t^*$) is given by the linear sum of two wave components: a sub-k_m^* and a super-k_m^* component. At the limits, the sub-k_m^* components merge with pure capillary waves, and the super-k_m^* components with the pure gravity waves.

(vi) Most of the energy imparted by the drop to the initially quiescent body of

water is in the capillary range. However, the corresponding waves are damped very rapidly with distance and can only be observed near the drop.

(vii) At a short distance from the drop (< 20 cm) (and small time after impact), the super-k_m^* components have a relatively large amplitude. They precede and hide the sub-k_m^* components.

(viii) At a large distance (> 60 cm) (and larger time), the super-k_m^* components are damped rapidly and only the sub-k_m^* components remain visible.

(ix) The wave amplitude is proportional to the momentum of the falling object, M^*W^*, i.e. proportional to $R^{*3}W^*$, which is $R^{*3.5}$ in the case where W^* reaches terminal velocity and $R^* > 1$ mm.

(x) Only the larger drops ($R^* > 1$ mm) are able to impart enough visible energy in the sub-k_m^* range, and the resulting rings cover a visibly large area ($r^* > 1$ m). The smaller drops ($R^* < 1$ mm) cause visible rings in the super-k_m range, which can be observed near the drop location only ($r < 20$ cm).

(xi) Since the drop size is limited by air pressure forces to a maximum value of about 3 to 4 mm and since drops that are smaller than 1 mm cause rings of very limited visible size, it appears that the prevailing sea state generated by intense rain ($R^* > 2$ mm) can be described by a relatively narrow energy spectrum peaked near k_m^*, of sub-k_m^* components.

(xii) The trailing wave has the highest wave crest and is terminated by a rapidly decaying elevation towards the drop location. The free-surface elevation at $r^* = V_m^* t$ is finite. Inside that ring ($r^* < r_m^*$), the free surface is practically quiescent.

(xiii) An accurate assessment of the free-surface film contamination and dissipative processes is paramount to an accurate determination of the wave amplitude and wave steepness.

This study was partly sponsored by the US Army Corps of Engineers under subcontract with the Defense Nuclear Agency. The author acknowledges Drs Mike Brown, Richard Skop and Shen Wang for many useful discussions during the course of this investigation.

REFERENCES

Abramovitz, M. & Stegun, I. A. 1965 *Handbook of Mathematical Functions.* Dover.

Crapper, G. D. 1984 *Introduction to Water Waves.* Wiley.

Dorrestein, R. 1951 General linearized theory of the effect of surface films on water ripple. *Ken. Ned. Akad. Wet. B.* **54**, 260–272.

Gunn, R. & Kinzer, G. D. 1949 The terminal velocity of fall of water droplets in stagnant air. *J. Met.* **6**, 243–248.

Horton, R. E. 1948 Statistical distribution of drop sizes and the occurrence of dominant drop sizes in rain. *Trans. Am. Geophys. Un.* **29**, 624–630.

Jeffreys, H. & Jeffreys, B. S. 1956 *Methods of Mathematical Physics.* Cambridge University Press.

Kajiura, K. 1963 The leading wave of a tsunami. *Bull. Earthquake Res. Inst.* **41**, 535–571.

Kranzer, H. C. & Keller, J. B. 1950 Water waves produced by explosion. *J. Appl. Phys.* **30**, 398–407.

Lamb, H. 1932 *Hydrodynamics.* Cambridge University Press.

Le Méhauté, B. 1970 Explosion generated water waves. *8th Symp. on Naval Hydrodynamics*, pp. 71–91. ONR.

Le Méhauté, B., Wang, S. & Lu, C. C. 1987 Spikes, domes and cavities. *J. Intl. Assoc. Hydraul. Res.* **5**, 583–602.

LHERMITTE, R. M. 1971 Probing of atmospheric motion by airborne pulse-doppler radar techniques. *J. Appl. Met.* **10**, 234–246.

PHILLIPS, O. M. 1966 *The Dynamics of the Upper Ocean.* Cambridge University Press.

VAN DORN, W. G. 1966 Boundary dissipation of oscillatory waves. *J. Fluid Mech.* **24**, 769–779 and Corrigenda **32** (1968), 828–829.

WHITHAM, G. B. 1974 *Linear and Nonlinear Waves.* Wiley-Interscience.